Hindawi
International Journal of Antennas and Propagation
Volume 2020, Article ID 6109093, 9 pages
https://doi.org/10.1155/2020/6109093

Research Article

A Novel Dual-Band Binary Branch Fractal Bionic Antenna for Mobile Terminals

Xiaoying Ran,[1] **Zhen Yu**,[1] **Tangyao Xie**,[2] **Yao Li**,[1] **Xiuxia Wang**,[3] **and Peng Huang**[4]

[1]*North China Institute of Science and Technology, Langfang, China*
[2]*Beijing HCD Technology Co., Ltd., Beijing, China*
[3]*Zhejiang Sci-Tech University, Hangzhou, China*
[4]*Hangzhou Dianzi University, Hangzhou, China*

Correspondence should be addressed to Zhen Yu; yzyuzhen@ncist.edu.cn

Received 29 July 2019; Revised 25 October 2019; Accepted 22 November 2019; Published 9 January 2020

Academic Editor: Shah Nawaz Burokur

A novel two-iteration binary tree fractal bionic structure antenna is proposed for the third generation (3G), fourth generation (4G), WLAN, and Bluetooth wireless applications in the paper, which is based on the principles of conventional microstrip monopole antenna and resonant coupling technique, combined with the advantages of fractal geometry. A new fractal structure was presented for antenna radiator, similar to the tree in nature. The proposed antenna adapted two iterations on a fractal structure radiator, which covers mobile applications in two broad frequency bands with a bandwidth of 44.2% (1.85–2.9 GHz) for TD-SCDMA, WCDMA, CDMA2000, LTE33-41, and Bluetooth frequency bands, and 11.5% (4.9–5.5 GHz) for WLAN frequency band. The proposed antenna was fabricated on a G10/FR4 substrate with a dielectric constant of 4.4 and a size of 50×40 mm^2. The good agreement between the measurement results and the simulation results validate that the proposed design approach meet the requirements for various wireless applications.

1. Introduction

In recent years, due to the rapid development in wireless communication technology and applications, the demand for multiband wireless mobile terminals has been increasing. Therefore, it is necessary to design the multiband, compact, low profile, and low-cost antennas, and many types of antennas have been proposed to achieve multiband functions. In addition, wideband properties in resonance characteristics of monopole and dipole antennas have been broadly investigated over the years using various techniques [1, 2].

Various methods have been studied to obtain multiband enhancement, including slot-loaded technologies [3–5], coupling feed technologies [6, 7], loading the matching network [8], and fractal technologies [9]. The desired resonant frequency band is produced by controlling the current path and resonant mode of the antenna radiator. Alternatively, multiple monopole or dipole antennas may be employed as resonant branches having different operating frequencies to create multiple operating bands. In [10], the coupling branches or parasitic patches are isolated from the antenna, and the electromagnetic coupling between them is used to achieve multiband capabilities. In [11], slots are etched on the radiator to change the local current mode and produce different resonance frequencies.

At the same time, with the miniaturization of the terminal device, the radiator is usually bent and folded to increase the antenna electrical length to make the antenna operate at lower frequencies [12]. The bending and folding method of the antenna radiator structure is used to increase the electrical length of the antenna to achieve miniaturization of the antenna [13–15]. Among these design methods, fractal structure approaches are the most representative for their compact size, low profile, and multiband response, with

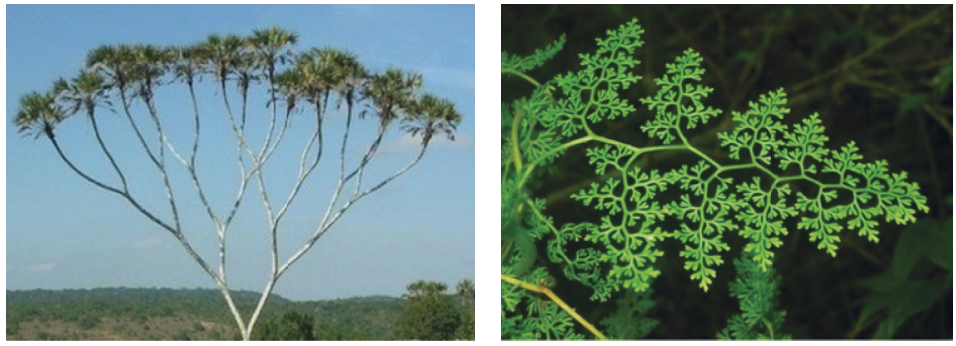

(a) (b)

Figure 1: Binary branches in nature.

fractal self-similarity and space filling used to increase the antenna electrical length and radiation efficiency [16–18].

From another perspective, the self-similarity of the fractal structure can be regarded as the genetic property of biology, that is, it has certain biomimetic structural characteristics. Most of the literatures use traditional structures such as Koch, Box, Sierpinski, Cantor, and Mandelbrot fractal, for the application of fractal structures in antenna engineering, but less research studies on fractal structures with biomimetic features. In [19–24], the appearance of octopus shape, ginkgo leaf shape, butterfly shape, tree structure, ancient coin-like structure, and curved branch tree are integrated into the antenna design. In [25], it presents a new planar antipodal Vivaldi antenna with nature fern-leaf inspired fractal structure which is around 19.7 GHz starting from 1.3 to 20 GHz.

In this work, the fractal structure of the binary genetic characteristics in nature is improved and applied to the antenna radiator structure design. A novel dual-band broadband antenna with a bionic fractal structure for dual-broadband mobile terminal is presented. The antenna covers mobile applications of TD-SCDMA (1880–2025 MHz), WCDMA (1920–2170 MHz), CDMA2000 (1920–2125 MHz), LTE33-41 (1900–2690 MHz), Bluetooth (2400–2483.5 MHz), and WLAN (802.11a/b/g/n: 2.4–2.48 GHz, 5.15–5.35 GHz) system.

2. Antenna Structure and Design Procedure

2.1. Characteristics of the Antenna Structure. In order to obtain more sunlight energy, plants in nature continue to grow to make full use of space and exhibit obvious genetic fractal characteristics in appearance. For antennas in a limited space, in order to improve the efficiency of radiating and receiving electromagnetic waves, the spatial filling of the fractal geometry can be used to increase the length of the radiator in a limited space. The binary geometry of nature is applied to the antenna engineering in the paper. Based on the binary tree, the binary branching is performed on each branch, and the structure is proposed as the antenna radiator after two iterations, as shown in Figure 1.

The proposed planar antenna structure is shown in Figure 2 with dimensions in Table 1. The antenna has a two-iteration binary branches fractal structure. Miniaturization and multiband coverage are achieved by varying the length of the antenna surface current flow and through. The antenna is designed on FR4 substrate. A 50 Ω ladder structure coplanar waveguide structure feed line is used to extend the bandwidth, and the overall size is $50 \times 40 \times 1.6\,\text{mm}^3$.

2.2. Simulation Results of the Antenna. Simulations are conducted using the Ansoft HFSS software package. The basic shape of the antenna radiator is a V-shaped structure with an opening angle of 90 degrees, and the fractal is taken at 1/3 of the outermost side length, and then the fractal is performed once again at 1/3 of the length of each branch side. The evolution process is shown in Figure 3. The orange section is the copper radiator and the coplanar waveguide structure grounding plate, the green section is the dielectric material.

V-shape radiator performance with different line widths are compared, and 1 mm is selected as the line width of the basic antenna radiator (no iteration), as shown in Figure 4.

The reflection loss of the no iteration antenna is lower than that of the higher iteration fractal antennas, but the working frequency band coverage is not as good as that of the higher iteration fractal antennas, as shown in Figure 5. The red solid line shows that the proposed antenna operates at two different wide frequency bands with three resonance frequencies centred at 2 GHz with a −18.1 dB return loss, 3.25 GHz with a −19 dB return loss, and 5.1 GHz with a −12.7 dB return loss. The simulated −10 dB return loss bandwidth is 71.2% for the first frequency band (1.7–3.58 GHz) and 22.2% for the second band (4.8–6 GHz). These bands cover several commercial application bands for the 3G, 4G, WLAN, and Bluetooth system technologies (see Table 2).

The simulated 3D gain and far-field normalized E/H-plane radiation patterns of the proposed antenna at the centre frequencies of 2, 3.25, and 5.1 GHz with peak gains of 2.3, 4.1, and 3 dBi are shown in Figures 6 and 7, respectively. The E- and H-plane patterns are omnidirectional at the low band and close to omnidirectional at all other bands, as the higher-order modes produce nulls

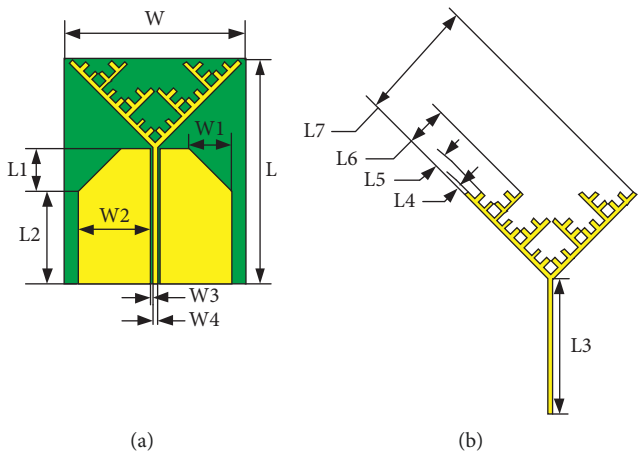

Figure 2: Layout of the proposed binary tree fractal antenna.

Table 1: Dimensional of the proposed antenna.

W	W1	W2	W3	W4	L	L1	W	L2	L3	L4	L5	L6	L7	L2
40	9.5	16.5	1	0.5	50	9.5	40	20.5	30.5	1	2	8	26	20.5

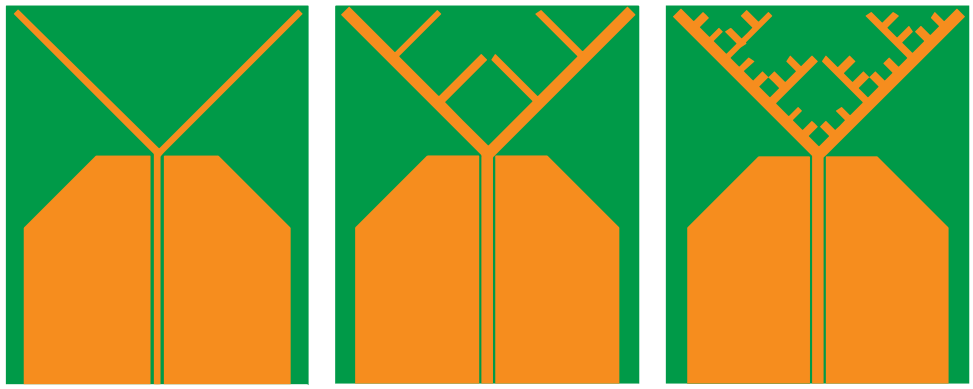

Figure 3: Proposed antenna in the stepwise iteration stages. (a) No iteration. (b) 1st iteration. (c) 2nd iteration.

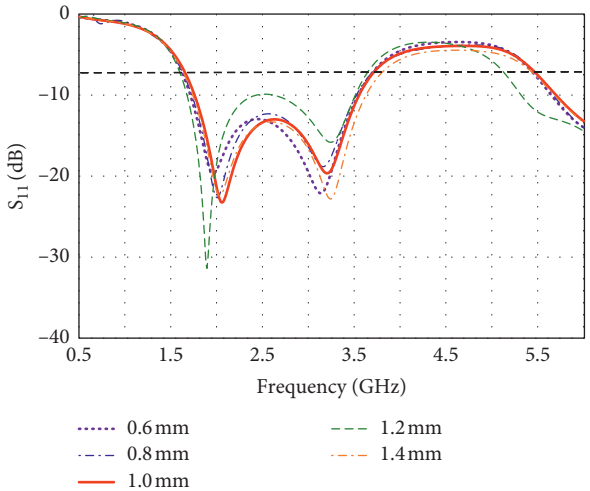

Figure 4: Performance comparison of basic radiators with different line widths.

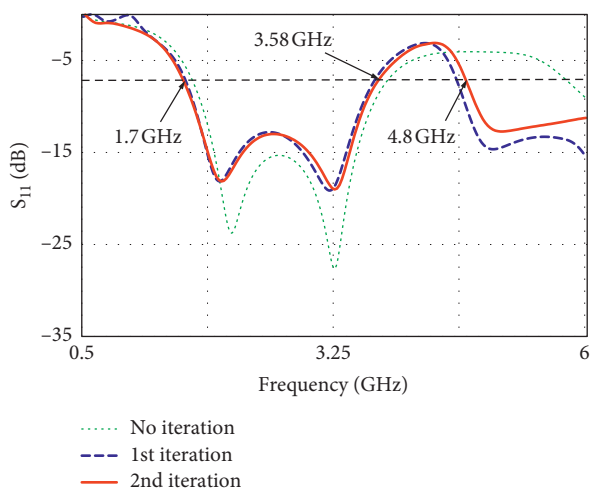

Figure 5: Combined simulated return loss for the antenna iterations.

Table 2: Frequency bands covered by the antenna.

Frequency band	Bandwidth	Commercial channel coverage
1	1.7–3.58 GHz (71.2%)	TD-SCDMA (1,880–2,025 MHz, 2,300–2,400 MHz supplementary), WCDMA (1,920–2,170 MHz, 1,755–1,880 MHz supplementary), CDMA2000 (1,920–2,125 MHz), LTE33-41 (1,900–2,690 MHz), Bluetooth (2,400–2,483.5 MHz), and WLAN (802.11 b/g/n: 2.4–2.48 GHz)
2	4.8–6 GHz (22.2%)	WLAN (802.11a/n: 5.15–5.35 GHz)

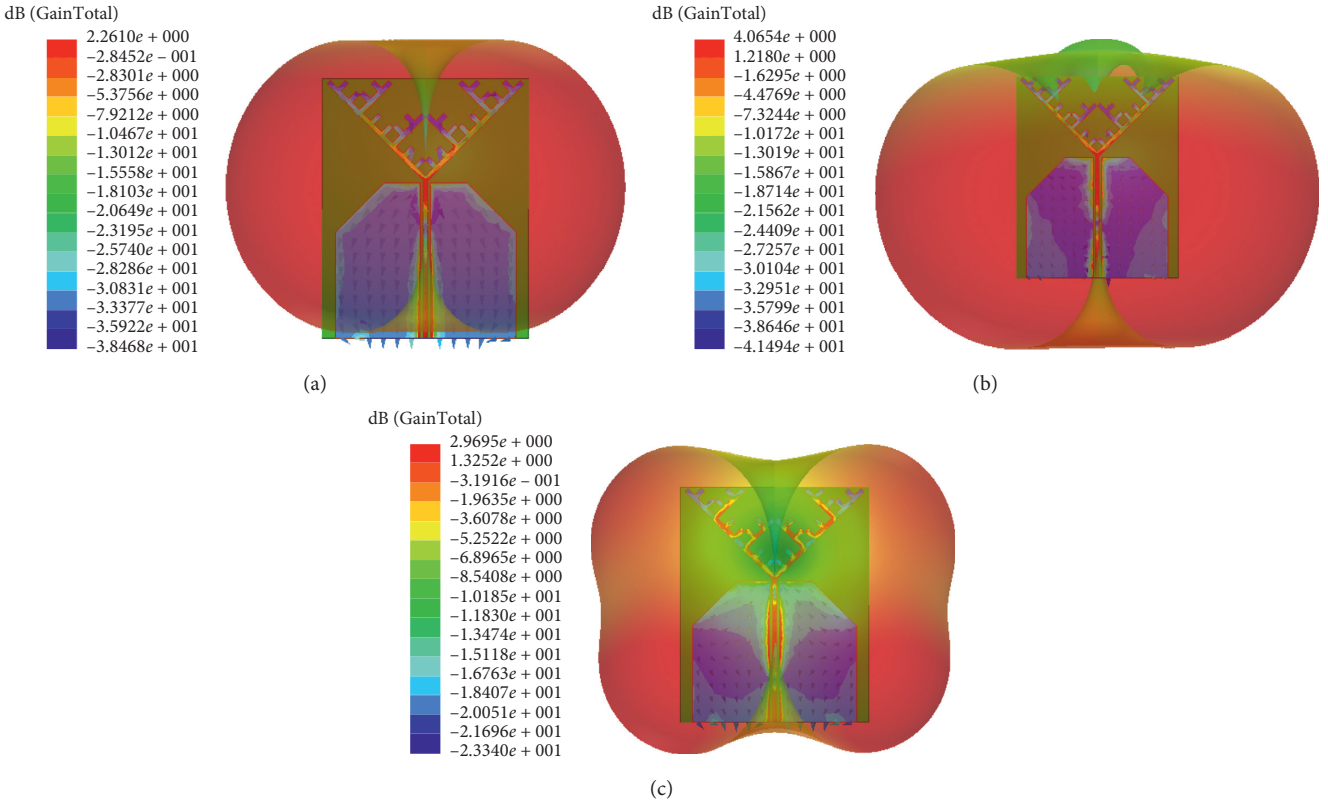

Figure 6: 3D radiation patterns. (a) 2 GHz. (b) 3.25 GHz. (c) 5.1 GHz.

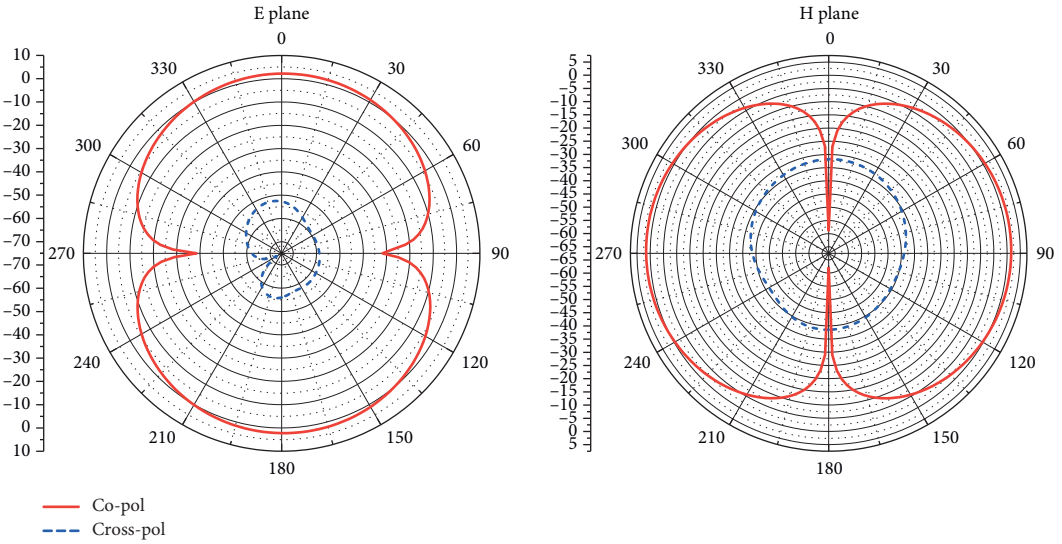

Figure 7: Continued.

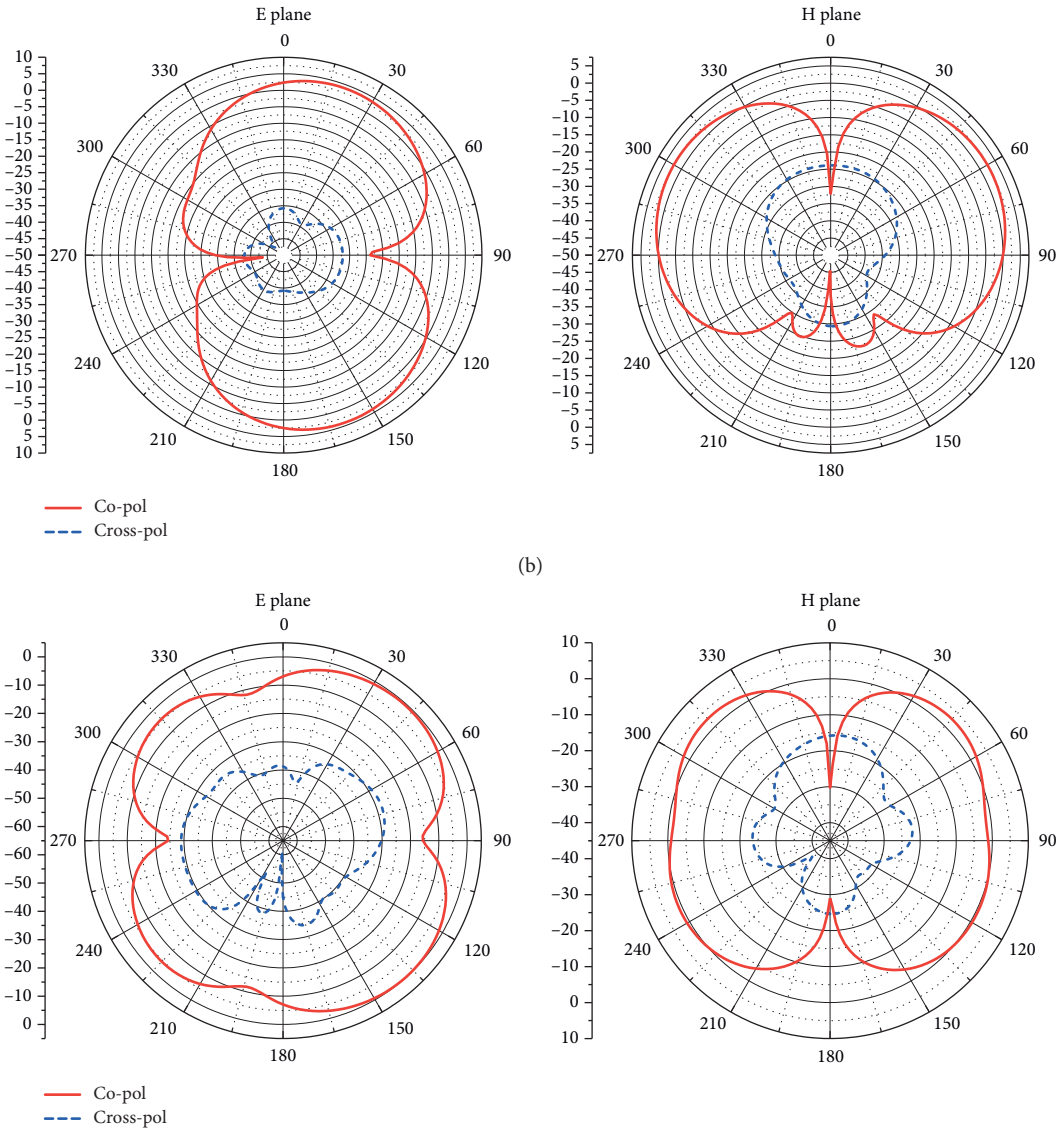

Figure 7: E- and H-plane radiation patterns. (a) 2 GHz. (b) 3.25 GHz. (c) 5.1 GHz.

and side lobes, and low level of cross polarization is obtained.

The surface current amplitude and vector distribution on the conducting part of the proposed antenna at centre frequencies of 2, 3.25, and 5.1 GHz are shown in Figure 8. For the 2 GHz frequency band, the outer edges of the monopole have more current (see Figure 8(a)). As the frequency increases, the current becomes more concentrated at the inner iteration surface. For the 5.1 GHz frequency band, the current reaches a relative maximum at the edges of the radiator (see Figure 8(c)).

3. Prototype and Measured Results

The prototype of the antenna is built on a 1.6 mm thick FR4 substrate with dielectric constant (ε_r) of 4.4 and loss tangent (δ) of 0.02 and copper on both sides, as shown in Figure 9. The antenna was tested by Satimo antenna measurement system SG24 in anechoic chamber and the test antenna was a dual-polarized horn antenna with a gain of 4–12 dBi. We used the same test process and analysis method as the two papers published [18, 24].

The comparison of the measurement return loss and the simulation result is shown in Figure 10. The measured −10 dB bandwidths of the antenna are 1.85–2.9 GHz and 4.9–5.5 GHz, the return loss at the centre resonance frequency of 2.3 GHz is −23.8 dB, the return loss at 2.75 GHz is −23.8 dB, the return loss at 5.2 GHz is −16.3 dB, and the measured bandwidth of the antenna is matched with the simulated bandwidth. The antenna can cover wireless applications such as TD-SCDMA, WCDMA, CDMA2000, LTE33-41, Bluetooth, and WLAN, as shown in Table 3. Due

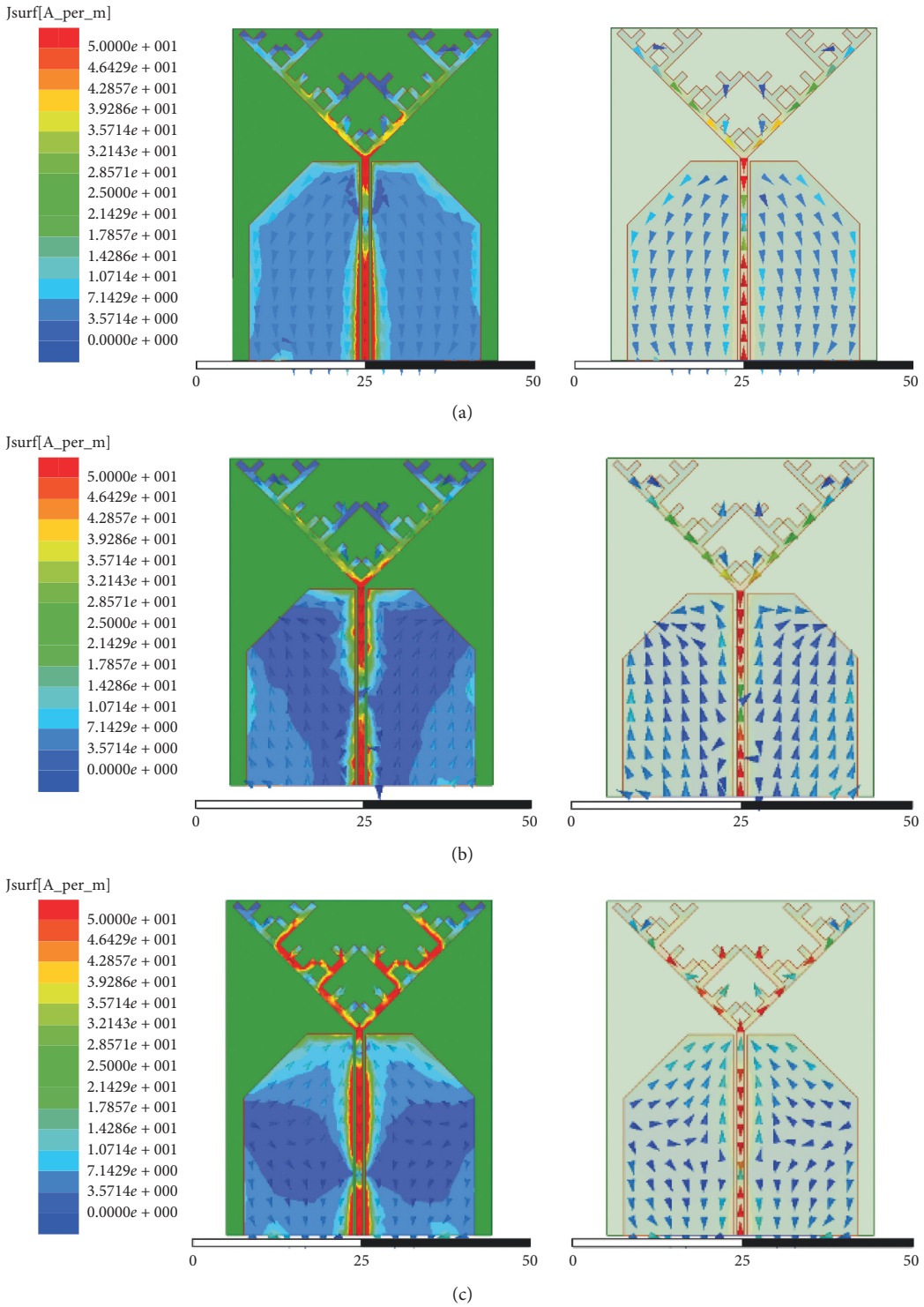

Figure 8: Surface current distribution in triple band modes. (a) 2 GHz. (b) 3.25 GHz. (c) 5.1 GHz.

to the fabrication accuracy of the antenna, the fabrication of the joint and the test error, there is a certain error between the test and the simulation data.

The measured 3D radiation pattern at the centres of the 2, 3.25, and 5.1 GHz resonance points is shown in Figure 11.

Compared with the simulation graphs, the antenna has good omnidirectional radiation characteristics in all frequency bands. As the frequency increases, the side lobes gradually appear, but the zero point still does not appear; in addition, the measurement results are in good agreement with the simulation results.

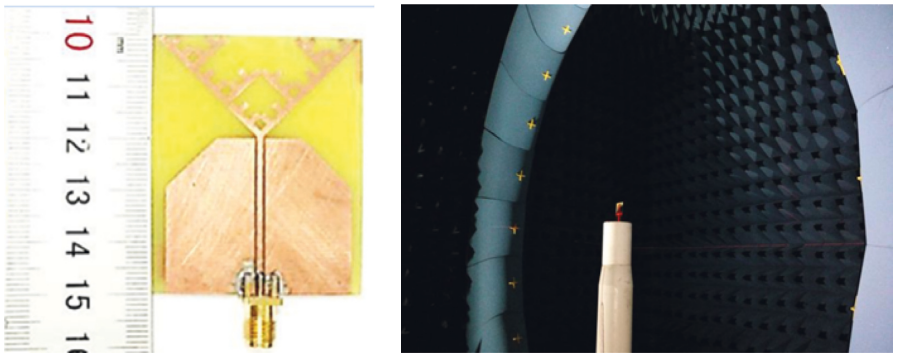

(a) (b)

Figure 9: Prototype of the antenna and test scenario in anechoic chamber.

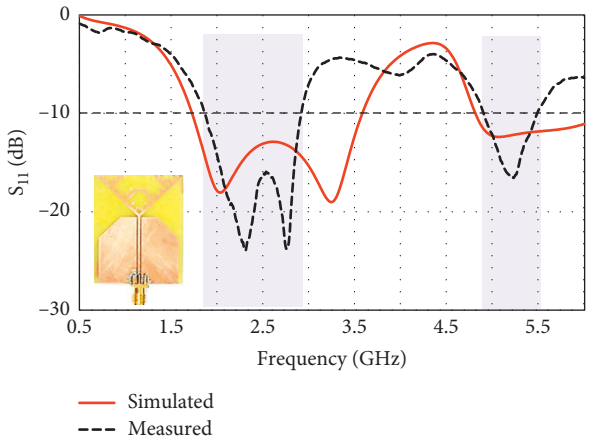

Figure 10: Measured and simulated S11 of the antenna.

Table 3: Measured frequency bands of the antenna.

Frequency band	Bandwidth	Commercial band coverage
1	1.85–2.9 GHz (44.2%)	TD-SCDMA (1880–2025 MHz, 2300–2400 MHz supplementary), WCDMA (1920–2170 MHz), CDMA2000 (1920–2125 MHz), LTE33-41 (1900–2690 MHz), Bluetooth (2400–2483.5 MHz), and WLAN (802.11 b/g/n: 2.4–2.48 GHz)
2	4.9–5.5 GHz (11.5%)	WLAN (802.11a/n: 5.15–5.35 GHz)

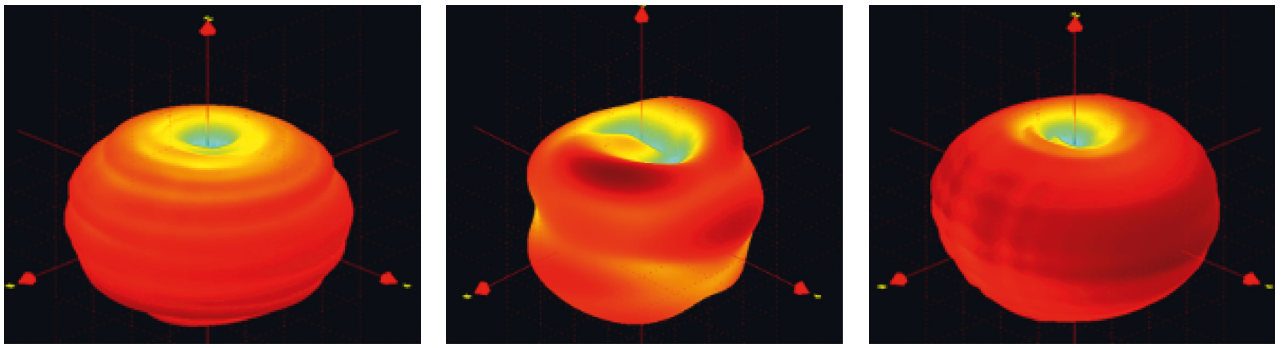

(a) (b) (c)

Figure 11: Measured 3D radiation patterns. (a) 2 GHz. (b) 3.25 GHz. (c) 5.1 GHz.

4. Conclusions

This work developed a 2 iterations binary tree fractal bionic structure dual-broadband planar antenna for CDMA, LTE, Bluetooth, and WLAN applications. The multiband antenna covers two broadbands with a bandwidth of 44.2% (1.85–2.9 GHz) for TD-SCDMA, WCDMA, CDMA2000, LTE33-41, and Bluetooth frequency bands, and 11.5% (4.9–5.5 GHz) for WLAN frequency band. The measured results reveal omnidirectional radiation patterns. The good agreement between the measurement results and the simulation results validate that the proposed design approach meet the requirements for various wireless applications.

Data Availability

The simulation and test data used to support the findings of this study are included within the article.

Conflicts of Interest

The authors declare that there are no conflicts of interest.

Acknowledgments

This work was supported in part by the National Natural Science Foundation of China (grant no. 61663014), Science and Technology Research Project for Colleges and Universities of Hebei Province (grant no. Z2017133), Hebei Higher Education Teaching Reform Project (grant no. 2018GJJG477), Fundamental Research Funds for the Central Universities (grant nos. 3142018047 and 3142017073), and Key Laboratory of Coal Mine Safety Monitoring and Control Technology Safety Production (grant no. 3142018048).

References

[1] C. Goswami, R. Ghatak, and D. R. Poddar, "Multi-band bisected Hilbert monopole antenna loaded with multiple subwavelength split-ring resonators," *IET Microwaves, Antennas & Propagation*, vol. 12, no. 10, pp. 1719–1727, 2018.

[2] S. Verma and P. Kumar, "Compact triple-band antenna for WiMAX and WLAN applications," *Electronics Letters*, vol. 50, no. 7, pp. 484–486, 2014.

[3] T. Dabas, B. K. Kanaujia, D. Gangwar, A. K. Gautam, and K. Rambabu, "Design of multiband multipolarised single feed patch antenna," *IET Microwaves, Antennas & Propagation*, vol. 12, no. 15, pp. 2372–2378, 2018.

[4] Z. Chen, Y. L. Ban, J. H. Chen, J. L. W. Li, and Y. J. Wu, "Bandwidth enhancement of LTE/WWAN printed mobile phone antenna using slotted ground structure," *IEEE Antennas and Wireless Propagation Letters*, vol. 17, no. 8, pp. 1557–1560, 2018.

[5] M. T. Wu and M. L. Chuang, "Multibroadband slotted bowtie monopole antenna," *IEEE Antennas and Wireless Propagation Letters*, vol. 17, no. 2, pp. 331–334, 2018.

[6] M. E. Yassin, H. A. Mohamed, E. A. F. Abdallah, and H. S. El-Hennawy, "Single-fed 4G/5G multiband 2.4/5.5/28 GHz antenna," *IET Microwaves, Antennas & Propagation*, vol. 13, no. 3, pp. 286–290, 2019.

[7] K. S. Vishvaksenan, K. Mithra, R. Kalaiarasan, and K. S. Raj, "Mutual coupling reduction in microstrip patch antenna arrays using parallel coupled-line resonators," *IEEE Antennas and Wireless Propagation Letters*, vol. 16, pp. 2146–2149, 2017.

[8] P. M. Paul, K. Kandasamy, and M. S. Sharawi, "A triband circularly polarized strip and SRR-Loaded slot antenna," *IEEE Transactions on Antennas and Propagation*, vol. 66, no. 10, pp. 5569–5573, 2018.

[9] V. Sharma, N. N. Lakwar, T. Kumar, and T. Garg, "Multiband low-cost fractal antenna based on parasitic split ring resonators," *IET Microwaves, Antennas & Propagation*, vol. 12, no. 6, pp. 913–919, 2018.

[10] I. B. Issa and M. Essaaidi, "A novell compact multiband broadside-coupled split-ring-resonator metamaterial structure loaded fractal slot antenna for 4G communications and wireless systems," *Microwave and Optical Technology Letters*, vol. 58, no. 12, pp. 2823–2828, 2016.

[11] N. T. Thanh, Y. Yang, K. Y. Lee, and K. C. Hwang, "Dual circularly-polarized spidron fractal slot antenna," *Electromagnetics*, vol. 37, no. 1, pp. 40–48, 2017.

[12] S. Subbaraj, P. Sambandam, M. Kanagasabai et al., "Performance enhancement and signal integrity analysis of multiband MIMO antenna for handheld electronic devices," *IET Microwaves, Antennas & Propagation*, vol. 13, no. 5, pp. 631–641, 2019.

[13] A. Hamani, M. C. E. Yagoub, T.-P. Vuong, and R. Touhami, "A novel broadband antenna design for UHF RFID tags on metallic surface environments," *IEEE Antennas and Wireless Propagation Letters*, vol. 16, no. 1, pp. 91–94, 2017.

[14] W. Xiao, T. Mei, Y. Lan, Y. Wu, R. Xu, and Y. Xu, "Triple band-notched UWB monopole antenna on ultra-thin liquid crystal polymer based on ESCSRR," *Electronics Letters*, vol. 53, no. 2, pp. 57-58, 2017.

[15] Z. Hu, Y. Hu, Y. Luo, and W. Xin, "Modified sierpinski fractal UWB antenna with band-notched characteristic," *Journal of Electronics and Information Technology*, vol. 39, no. 6, pp. 1520–1524, 2017.

[16] J. S. Khinda, M. R. Tripathy, and D. Gambhir, "Multi-edged wide-band rectangular microstrip fractal antenna array for C- and X-band wireless applications," *Journal of Circuits Systems and Computers*, vol. 26, no. 4, Article ID 1750068, 2017.

[17] D. Shamvedi, O. J. McCarthy, E. O'Donoghue, P. O'Leary, and R. Raghavendra, "Improving the strength-to-weight ratio of 3-D printed antennas: metal versus polymer," *IEEE Antennas and Wireless Propagation Letters*, vol. 17, no. 11, pp. 2065–2069, 2018.

[18] Z. Yu, J. Yu, X. Ran, and C. Zhu, "A novel Koch and Sierpinski combined fractal antenna for 2G/3G/4G/5G/WLAN/navigation applications," *Microwave and Optical Technology Letters*, vol. 59, no. 9, pp. 2147–2155, 2017.

[19] W. Jiang, S.-X. Gong, T. Hong, and X. Mu, "Printed L-band monopole antenna with a bionical structure," *Microwave and Optical Technology Letters*, vol. 53, no. 5, pp. 1004–1006, 2011.

[20] Z. Zhang, "The design of a bionic antenna," *Journal of Xinjiang Normal University*, vol. 33, no. 1, pp. 33–40, 2012.

[21] J. Z. Sun and X. Chen, "Butterfly bionic antenna with ultra-wideband property," *Modern Electronics Technique*, vol. 36, no. 7, pp. 94–96, 2013.

[22] X. Y. Zhao, H. M. Zang, G. L. Zhang, and J. J. Lu, "A novel ultra-wideband fractal tree-shape antenna," *Journal of Electronics and Information Technology*, vol. 37, no. 4, pp. 1008–1012, 2015.

[23] X. Zeng, C. Zhang, Y. Wang, and C. Xie, "A novel planar tree-shaped fractal dipole patch antenna," *Telecommunication Engineering*, vol. 50, no. 5, pp. 76–79, 2010.

[24] Z. Yu, J. Yu, X. Ran, and C. Zhu, "A novel ancient coin-like fractal multiband Antenna for wireless applications," *International Journal of Antennas and Propagation*, vol. 2017, Article ID 6459286, 10 pages, 2017.

[25] B. Biswas, R. Ghatak, and D. R. Poddar, "A fern fractal leaf inspired wideband Antipodal Vivaldi antenna for microwave imaging system," *IEEE Transactions on Antennas and Propagation*, vol. 65, no. 11, pp. 6126–6129, 2017.